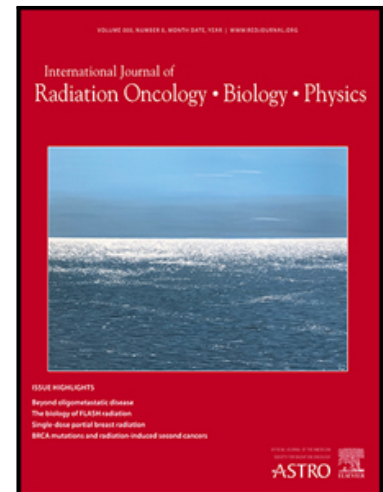


Journal Pre-proof

The Impact of Tumor Treating Fields on Glioblastoma Progression Patterns

Martin Glas , Matthew T. Ballo , Ze'ev Bomzon , Noa Urman , Shay Levi , Gitit Lavy-Shahaf , Suriya Jeyapalan , Terence T. Sio , Paul M. DeRose , Martin Misch , Sophie Taillibert , Zvi Ram , Andreas F. Hottinger , Jacob Easaw , Chae-Yong Kim , Suyash Mohan , Roger Stupp

PII: S0360-3016(21)03424-6
DOI: <https://doi.org/10.1016/j.ijrobp.2021.12.152>
Reference: ROB 27386



To appear in: *International Journal of Radiation Oncology, Biology, Physics*

Received date: 12 August 2021
Revised date: 6 December 2021
Accepted date: 15 December 2021

Please cite this article as: Martin Glas , Matthew T. Ballo , Ze'ev Bomzon , Noa Urman , Shay Levi , Gitit Lavy-Shahaf , Suriya Jeyapalan , Terence T. Sio , Paul M. DeRose , Martin Misch , Sophie Taillibert , Zvi Ram , Andreas F. Hottinger , Jacob Easaw , Chae-Yong Kim , Suyash Mohan , Roger Stupp , The Impact of Tumor Treating Fields on Glioblastoma Progression Patterns, *International Journal of Radiation Oncology, Biology, Physics* (2021), doi: <https://doi.org/10.1016/j.ijrobp.2021.12.152>

This is a PDF file of an article that has undergone enhancements after acceptance, such as the addition of a cover page and metadata, and formatting for readability, but it is not yet the definitive version of record. This version will undergo additional copyediting, typesetting and review before it is published in its final form, but we are providing this version to give early visibility of the article. Please note that, during the production process, errors may be discovered which could affect the content, and all legal disclaimers that apply to the journal pertain.

© 2021 Published by Elsevier Inc.

The Impact of Tumor Treating Fields on Glioblastoma Progression Patterns**Running Title:** GBM progression patterns with TTFields

Martin Glas^{1,*}, Matthew T. Ballo^{2,*}, Ze'ev Bomzon^{3*}, Noa Urman³, Shay Levi³, Gitit Lavy-Shahaf³, Suriya Jeyapalan⁴ Terence T. Sio⁵, Paul M. DeRose⁶, Martin Misch⁷, Sophie Taillibert⁸, Zvi Ram⁹, Andreas F. Hottinger¹⁰, Jacob Easaw¹¹, Chae-Yong Kim¹², Suyash Mohan¹³, and Roger Stupp¹⁴

* These three authors have contributed equally to this work

¹Division of Clinical Neurooncology, Dept. of Neurology and German Cancer Consortium (DKTK) Partner Site, University Hospital Essen, University Duisburg-Essen, Essen, Germany.

²Department of Radiation Oncology, West Cancer Center & Research Institute, Memphis,

TN. ³Novocure Ltd., Haifa, Israel. ⁴Tufts Medical Center, Boston, MA. ⁵Department of

Radiation Oncology, Mayo Clinic, Phoenix, AZ. ⁶Department of Radiation Oncology,

Methodist Dallas Medical Center, Dallas, TX. ⁷Department of Neurosurgery, University

Hospital Charité, Berlin, Germany. ⁸Department of Neurology, Hôpital Pitié-Salpêtrière,

APHP, University Pierre et Marie Curie Paris VI, Paris, France. ⁹Department of Neurosurgery,

Tel Aviv Medical Center, Tel Aviv, Israel and Tel Aviv University School of Medicine.

¹⁰Departments of Clinical Neurosciences and Oncology, Centre Hospitalier Universitaire

Vaudois, Lausanne, Switzerland. ¹¹Cross Cancer Institute, Edmonton, Canada. ¹²Seoul

National University Bundang Hospital, Seoul National University College of Medicine, Korea.

¹³Division of Neuroradiology, Department of Radiology, Perelman School of Medicine at the

University of Pennsylvania, Philadelphia, PA. ¹⁴Lou and Jean Malnati Brain Tumor Institute of

the Robert H. Lurie Comprehensive Cancer Center of Northwestern University, Departments

of Neurological Surgery, Neurology and Medicine (Hem/Onc), Northwestern Medicine,

Chicago, IL.

Corresponding Author:

Matthew T. Ballo, MD: Department of Radiation Oncology, West Cancer Center & Research Institute. 7945 Wolf River Blvd, Germantown, TN 38138. Phone: (901) 624-2600. E-Mail: mballo@westclinic.com

Author Responsible for Statistical Analyses:

Gitit Lavy-Shahaf: Biostatistics, Research and Development Novocure Inc. Topaz Building 4th Floor, MATAM Center P.O. Box 15022, Sh'ar HaCarmel, Haifa 31905, Israel. Phone: +972 053-2220816. E-Mail: glavy-shahaf@novocure.com

Conflict of Interest Statement:

Glas: MG received an honorarium from Novocure, is on Novocure advisory board and received funding from Novocure for a phase I/II trial. **Ballo**: MB does consulting for Novocure LLC and Zailab. **Bomzon**: ZB is a full-time employee of Novocure Ltd. and has equity in Novocure. **Urman**: NU is an employee of Novocure Inc. and has equity in Novocure. **Levi**: SL is an employee of Novocure Ltd. and has equity in Novocure. **Lavy-Shahaf**: GLS is an employee of Novocure Ltd. and has equity in Novocure. **Jeyapalan**: SJ is on the Novocure speaker bureau. **Sio**: TS is a member of Novocure advisory board and speaker bureau. **DeRose**: PD has no conflict of interest. **Misch**: MM has received a research grant, speaker's fee and travel costs from Novocure in the past. **Taillibert**: ST has no conflict of interest. **Ram**: ZR is a consultant for NovoCure Ltd. **Hottinger**: AFH received travel support for medical meeting to present trial results (paid to the institution). **Easaw**: JE has no conflict of interest. **Kim**: CYK has no conflict of interest. **Mohan**: SM, Consultant for Northwest Biotherapeutics, money paid to individual; grants/grants pending: Novocure, Galileo, money paid to institution. **Stupp**: RS was the principal investigator of the trial and received travel support for medical meetings to present trial results.

Funding: This study and the EF-14 trial [NCT00916409] was funded by Novocure.

Data Availability Statement: Research data are not available at this time.

Word Count:

Abstract – 275 words

Manuscript body – 3,489 words

Figure Legends – 258 words

References - 25

Journal Pre-proof

Abstract

Background: Tumor-treating fields (TTFields) is an antimitotic treatment modality that interferes with glioblastoma cell division and organelle assembly by delivering low-intensity alternating electric fields to the tumor. A previous analysis from the pivotal EF-14 trial demonstrated a clear correlation between TTFields dose-density at the tumor bed and survival in patients treated with TTFields. This study tests the hypothesis that the antimitotic effects of TTFields result in measurable changes in the location and patterns of progression of newly diagnosed glioblastoma (nGBM) patients.

Methods: MRI images of 428 nGBM patients that participated in the pivotal EF-14 trial were reviewed and the rates at which distant progression occurred in the TTFields treatment and control arm were compared. Realistic head models of 252 TTFields treated patients were created and TTFields intensity distributions were calculated using a Finite Elements Method. TTFields dose was calculated within regions of the tumor bed and normal brain and its relationship with progression determined.

Results: Distant progression was frequently observed in the TTFields-treated arm, and distant lesions in the TTFields-treated arm appeared at larger distances from the primary lesion than in the control arm. Distant progression correlated with improved clinical outcome in the TTFields patients, with no such correlation observed in the controls. Areas of normal brain that remained normal were exposed to higher TTFields doses compared to normal brain that subsequently exhibited neoplastic progression. Additionally, the average dose to areas of enhancing tumor that returned to normal was significantly higher than in the areas of normal brain that progressed to enhancing tumor.

Conclusions: There was a direct correlation between TTFields dose distribution and tumor response, confirming the therapeutic activity of TTFields and the rationale for optimizing

array placement to maximize TFields dose in areas at highest risk of progression, as well as array layout adaptation after progression.

Keywords: TFields, Glioblastoma, Tumor progression, TFields dose, MRI

Journal Pre-proof

Introduction:

Tumor Treating Fields (TTFields) are a cancer treatment modality that has shown efficacy in the treatment of glioblastoma (GBM) and mesothelioma and are being investigated in other solid tumors. TTFields are alternating electric fields with frequencies of 100-500 kHz delivered via transducer arrays placed on the skin overlying the tumor. TTFields exert an anti-mitotic effect on dividing cells by interfering with the spindle apparatus.¹⁻⁴ Preclinical studies have shown that the inhibitory effects of TTFields depend upon the frequency and intensity of the fields, and the duration of exposure. To maximize the clinical efficacy, the frequency of the field is set specifically to maximize the effect on the primary tumor type (e.g., GBM at 200 kHz). The placement of the arrays is customized to maximize field intensity at the tumor bed.^{5,6} Device usage (fraction of time on treatment) is automatically monitored aiming to achieve over 75% compliance that is associated with improved clinical outcomes.⁷

In a randomized phase 3 trial (EF-14), prolongation of progression-free and overall survival of adjuvant treatment with TTFields was demonstrated in newly diagnosed GBM patients.⁸ A post-hoc simulations-bases analysis of phase III trial data suggested a positive correlation between TTFields dose at the tumor bed and overall survival.⁹ Here we investigate the patterns of progression of the EF-14 trial patients treated with TTFields versus controls and analyze whether these progression patterns are associated with differences in TTFields dose distribution.

Methods and materials:

Data were collected from within the previously reported EF-14 trial (NCT00916409) that randomized 695 newly diagnosed GBM patients (2:1) after completion of chemoradiotherapy to TFields plus adjuvant temozolomide (TMZ) chemotherapy or TMZ alone.^{8,10} All patients in the EF-14 trial provided written informed consent, and the study was approved by the institutional review boards or ethics committees of all participating centers.

Patients in the EF-14 trial were randomized after the end of radiochemotherapy at a ratio of 2:1 to receive standard maintenance temozolomide chemotherapy (150-200mg/m²/d for 5 days every 28 days for 6cycles) with or without the addition of TFields. Tumor treating fields treatment (200-kHz) was to be initiated at least 4 weeks but not more than 7 weeks from the last day of radiotherapy. Maintenance temozolomide was delivered in 28-day cycles. TFields were delivered through 4 transducer arrays with 9 insulated electrodes each placed on the shaved scalp and connected to a portable device set to generate 200-kHz electric fields within the brain (Optune, Novocure Inc). Transducer array layouts were determined using a TFields mapping software system to optimize field intensity within the treated tumor (NovoTAL, Novocure Inc).

Patient imaging data for the analysis of progression

Magnetic resonance images (MRI) were acquired at baseline (4-7 weeks post-chemoradiation) and during follow-up every 2 months for the first 6 months, then every 3 months. All images were reviewed by an independent panel of neuroradiologists. For the current study we analyzed data of 428 (62%) patients who had progressed during the trial observation period and for whom imaging was available at both baseline and progression.

Figure 1 is a flowchart describing the number of patients included in each of the analyses described below.

Tumor segmentation

The progression T1 contrast enhanced images (T1c) MRI as determined by the independent radiological panel were registered to the baseline T1c MRI using the SPM 12 (2014) software package.¹¹ Volumes of enhancing tumor at both baseline and progression were manually segmented using ITK-SNAP.¹²

Progression Pattern Analysis of GBM patients treated with TTFields plus TMZ or TMZ alone

To test the hypothesis that progression patterns in patients treated with TTFields + TMZ differ from those in patients treated with TMZ alone, progression of enhancing tumor as contoured from the T1c MRI was classified as being either distant or local. There is no standard method for classifying progression as being distant, and a range of definitions for distant progression exist in the neuroimaging literature.¹³ In this study we analyzed progression patterns using two commonly used methods. For the first method, distant progression was defined as the appearance of a new lesion, not contiguous with all lesions visible at baseline.¹³ Local progression was defined as an increase in size of an existing lesion. For each patient the minimum distance from a primary lesion to any new lesions was measured. The rates of occurrence of distant progressions in the TTFields plus TMZ group and TMZ alone group were calculated, as were the rates of occurrence of progression in the infratentorial brain (a distinct form of distant progression). Identification of distant progression was performed automatically. Therefore, to ensure robust and consistent identification of distant progression whilst accounting for image resolution (~1 mm) and registration error (~1 mm), regions of progression were identified as being distant if the

distance between the enhancing edge of the new lesion and the enhancing edge of a lesion visible at baseline was greater than 3 mm.¹⁴

For the second method, we compared the rates at which new lesions appear outside of the 20 mm boundary zone around the primary lesion in the TTFIELDS plus TMZ and TMZ alone groups. This analysis was performed since distant progression is often defined as appearance of a new lesion outside the clinical target volume (CTV) which encompasses the gross tumor volume (GTV) and a 20 mm margin around the tumor and resection cavity.¹³ Comparisons between the TTFIELDS plus TMZ and TMZ alone groups were performed as described in the statistical analysis section below.

MGMT-methylation at the tumor is a known prognostic factor for GBM patients.¹⁵ It has also been demonstrated that MGMT-methylation influences progression patterns.¹⁶ Therefore, comparisons between the rates at which distant progressions (new regions of contrast not contiguous to the primary lesion) occurred in *MGMT*-methylated and *MGMT*-unmethylated patients were performed. Comparisons were performed for the entire EF-14 study population and for the TTFIELDS plus TMZ and TMZ alone groups.

To test the hypothesis that the location of progression was associated with patient outcome, Kaplan-Meier curves were used to compare PFS and OS in patients that did and did not exhibit distant progression. This analysis was performed separately for each of the TTFIELDS plus TMZ and the TMZ alone groups.

Throughout the text, unless explicitly stated otherwise, distant progression refers to the appearance of a new lesion not contiguous to the primary lesion. We note that patients could exhibit both local and distant progression simultaneously.

Calculating TFields dose and its effect on GBM progression

To test the hypothesis that progression patterns are associated with differences in TFields dose distribution, we first selected patients from the TFields plus TMZ group to ensure that changes in progression could be associated with a minimum duration of TFields treatment. Therefore, only patients who were on treatment for more than two months were included in this analysis (n=30 of the 306 TFields patients were treated for < 2 months and were excluded from this portion of the study). Patients whose MRI quality was insufficient for model creation (N=24) were also excluded. Realistic computational head models of the remaining patients (N=252) were created from the T1c MRI scans at baseline and TFields intensity distributions within their brains were calculated as previously described.¹⁷ To model delivery of TFields, additional data were collected from the Optune™ device used to provide TFields therapy during the EF-14 trial. These data included the patient's average monthly device usage, and the average electrical current delivered to each patient as downloaded from the memory banks of their device. In addition, the transducer array layouts as documented in the patient's clinical record was also collected. To clarify, prior to starting TFields treatment, a treatment plan depicting how transducer arrays should be placed on the scalp was generated for each patient in the TFields plus TMZ group. These treatment plans were used to optimize TFields delivery for each patient, specific to their tumor location. For all patients, TFields dose was calculated as the product of TFields intensity: E (V/cm) squared tissue conductivity: σ (Siemens/m), and the average device usage: U (hours/day) during the first 6 months of therapy.⁹

$$Dose = \frac{1}{2} \sigma E^2 \times U$$

For each patient, an expansion margin was added to the baseline resection cavity plus any residual gross tumor to define a peri-tumoral brain zone (PBZ). To account for

inherent uncertainty in the calculations, we added 5 variable PBZ expansion margins (3, 5, 10, 15, or 20 mm) and repeated the analysis for each volume to determine the sensitivity of the results. Four baseline-to-progression volumes were identified on T1c MRIs: (i) normal brain tissue within the PBZ that progressed to tumor tissue (norm to tumor); (ii) normal brain tissue within the PBZ that remained normal tissue (norm to norm), (iii) enhancing tumor that remained enhanced (tumor to tumor); and (iv) enhancing tumor that regressed to normal/necrotic tissue (tumor to norm). The average TTFields dose in each of these volumes was calculated and the average doses compared. The number of patients included in each analysis depended upon the number of patients exhibiting progression in the relevant volumes in their T1c MRIs.

Statistical analysis

Statistical analysis was performed using SAS 9.4. All analyses regarding the rate of occurrence of distant progressions were performed using chi-squared tests. The distances of new lesions from the primary lesions were analyzed using a Wilcoxon rank-sum test. The rates of occurrence of infratentorial progression (a special case of distant progression) were analyzed using a t-test. Overall survival (OS) and progression free survival (PFS) were calculated from time of randomization in the EF-14 trial – 4-7 weeks after the end of radiochemotherapy – to the OS or PFS event. The median OS and PFS for each progression pattern group were estimated from Kaplan-Meier curves; the P values of the differences in the curves were calculated using log-rank test. Hazard Ratios (HR) were calculated using a Cox proportional hazards model accounting for sex, age, KPS, country, and MGMT status. Comparisons between doses within regions of the PBZ were performed using t-tests.

Results

Changes in tumor growth patterns

The demographics of patients included in this study were well balanced between the TTFields plus TMZ and TMZ alone groups included in the progression pattern analysis (Table 1). These demographics did not differ substantially from the overall demographics of the EF-14 study population.⁸

Distant progressions, defined as new regions of contrast not contiguous to any primary lesions (1st method - the distance between the enhancing edge of the new lesion and the enhancing edge of a lesion visible at baseline was greater than 3 mm) were observed in 17% (21/122) of the TMZ alone group and 23% (71/306) of the TTFields plus TMZ treatment group ($p=0.17$), with no statistically significant difference between the groups. However, the median distance between primary and distant progressions was larger in the TTFields treatment arm than in the control (control: 14.2 ± 14.4 mm, TTFields 23.2 ± 29.8 mm, $p=0.03$). The rate at which distant lesions appeared outside the 20 mm margin surrounding the tumor and resection cavity (2nd method) was higher in the TTFields treatment arm than in the control (control: 8.2%, 10/122, TTFields: 17.3%, 53/306, $p<0.02$). In addition, infratentorial distant progressions were only observed in the TTFields treatment arm, with no cases in the control (control: 0%, 0/122, TTFields: 3.6%, 11/306, $p<0.001$).

Analyzing all patients as a single group showed that distant progression (new lesions not contiguous to the primary lesion) was more common in patients with *MGMT* methylated tumors (*MGMT* methylated: 30% (35/117) vs. *MGMT* unmethylated: 17.5% (37/212), $p=0.009$). Distant progression for *MGMT* methylated tumors was also analyzed in each treatment group separately; for TTFields plus TMZ (*MGMT* methylated: 33% (28/85) vs. *MGMT* unmethylated: 21.5% (32/149), $p=0.053$), and for TMZ alone (*MGMT* methylated 22% (7/32) vs. *MGMT* unmethylated: 8% (5/63), $p=0.053$). Comparison of distant

progression rates across subgroups revealed that *MGMT* unmethylated patients treated with TTFields plus TMZ were 13.5% more likely to exhibit distant progression compared to unmethylated patients in the TMZ alone group (chi square p-value=0.018). *MGMT* methylated patients treated with TTFields plus TMZ were 11% more likely to exhibit distant progression compared to methylated patients in the TMZ alone group (chi square p-value=0.24).

Patients that exhibited distant progression in the TTFields plus TMZ group had a significantly longer time to progression than patients in the same group that exhibited local progression (distant progression: n=71, 7.9 months, CI 6.1-10.8 months vs. local progression: n=235, 5.2 months, CI 4.4-5.9 months, HR=0.78, CI 0.59-1.03, p=0.012). The same analysis performed for patients in the TMZ alone group did not reveal differences in time to progression (distant progression: n=21, 3.8 months CI 2.2-4.0 months vs. local progression: n=101, 3.7 months, CI 2.1-9.5 months, HR=0.78, CI 0.46-1.36, p=0.26). There was a trend towards longer OS in TTFields-treated patients with distant progression compared to TTFields-treated patients that progressed locally (distant: n=71, 23.9 months CI 18.6-30.1 months vs. local: n=235, 18.8 months, CI 15.7-20.9 months, HR=0.81, CI 0.59-1.12, p=0.085). No such trend was observed within the TMZ alone group (distant progression: n=21, 11.3 months CI 8.9-18.6 months vs. local progression: n=101, 13.6-18.1 months, HR=1.22, CI 0.70-2.17, p=0.66). HRs calculated using Cox proportional hazards models confirmed that within the TTFields plus TMZ treated group, distant progression was independently associated with prolonged PFS. Kaplan-Meier curves summarizing the results in this section are shown in Figure 2.

Effects of TTFields dose on progression

Figure 3 shows MRI images at baseline and at progression as well as the calculated dose distribution maps for three representative patients. The various regions of the tumor have been marked on the images, as have regions of progression or regression within a 3mm PBZ around the primary tumor and resection cavity. In all patients shown in this figure, progression occurs in regions where the TTFields dose is relatively low, while regression occurs in regions where the dose is relatively high, supporting the hypothesis that progression patterns in TTFields patients is influenced by TTFields dose distribution.

In patients treated with TTFields for more than two months, the average TTFields dose in areas of normal brain that remained normal (norm to norm) at the time of progression was significantly higher than the average TTFields dose in areas of normal brain that progressed to tumor (norm to tumor). This result held regardless of the PBZ expansion margin used for the analysis (Table 2). Further analysis shows at the average TTFields dose in areas of enhancing tumor that regressed to normal (tumor to norm) was significantly higher than the average in the volume of normal brain that progressed to enhancing tumor (norm to tumor) (N=197, 0.83 mW/cm^3 vs 0.71 mW/cm^3 , $p < 0.001$). TTFields dose was also higher in the areas of tumor that regressed (tumor to norm) than in regions of tumor that remained enhancing (tumor to tumor) but the difference in average dose was not statistically significant (N=183, 0.82 mW/cm^3 vs 0.8 mW/cm^3 , $p = 0.09$).

Discussion

Since the late 1930s it has been known that GBMs present macroscopically and infiltrate outward from the visible tumor microscopically in a diffuse manner, the extent of which is difficult to appreciate until progression occurs.¹⁸⁻²⁰ Our results demonstrate a measurable effect of TTFields treatment on the pattern of tumor progression in newly

diagnosed GBM patients. Specifically, distant progression defined here as the appearance of a new lesion not contiguous to any existing lesion, is more common in patients treated with TTFields and TMZ when compared to adjuvant TMZ alone. In patients treated with TTFields, distant progression also correlates with improved clinical outcome. Our analysis demonstrated that areas of normal brain that remained normal with TTFields treatment received a higher dose of TTFields than areas of normal brain that progressed to visible tumor. This indicates that TTFields suppressed tumor growth in a dose-dependent manner.

This analysis showed that distant progression outside the 20 mm margin surrounding the primary lesion and the resection cavity was more common in the TTFields plus TMZ group than in the TMZ alone group. Furthermore, the distance between the primary and distant lesions was larger in the TTFields plus TMZ group. These observations strengthen the hypothesis that TTFields alter GBM progression through inhibition of local tumor growth. When local control is effective, and patient survival extended, distant progression may become more frequent as enough time lapses for cancer cells to form a new mass from either a pre-existing distant microscopic nidus or through migration of tumor cells away from the primary tumor site. Indeed, increased number of distant failures including tumor dissemination to the posterior fossa and brain stem has been observed in patients with longer overall survival.²¹

The rates of distant progression in patients reported in this study (8.2% of the TMZ alone group showed distant progression outside the 20 mm boundary zone) are comparable with rates of distant progression reported in other studies. For instance, Chan et al. reported a 9% failure rate at the margin of the high dose region in patients treated with dose escalation of radiotherapy (RT) to 90 Gy.²² Paulson et al. also reported about 9% distant failure outside a 20 mm boundary zone in patients treated with RT concurrent with

TMZ.²³ In their prospective study, the rate of distant failure did not depend on the expansion margins used to define the CTV. These studies suggest that in patients treated with RT+TMZ, the pattern of failure does not depend on the RT planning strategy. Interestingly, some studies have reported higher rates of distant progression in GBM patients treated with RT+TMZ. For instance, Gebhardt et al. reported distant progression in 28% of the cohort they analyzed.²⁴ Brandes et al. reported a similar rate of distant progression in the patient cohort they analyzed.²⁵ The higher rates of distant progression reported in these studies could in part be due to methodological differences in how distant progression was defined. Whereas we counted new lesions entirely outside of a 20 mm boundary zone for this analysis, Gebhardt et al. and Brandes et al. defined distant progression as progression for which at least 80% of the volume appears outside of the 95% isodose surface.^{24,25}

The results of this study show a connection between TTFIELDS dose distribution and tumor progression and response in patients treated with TTFIELDS for more than two months. Within this patient group, the average dose in regions of progression was significantly lower than in regions where regression or no radiological change were observed. Patients on treatment for less than two months were excluded from this study due to the assumption that such a short duration of treatment is not likely to elicit an effect on tumor progression. This assumption was supported by observations that response to TTFIELDS is often preceded by tumor growth during the first two months of treatment.²⁶

TTFIELDS may improve tumor control and patient outcome because of its regional rather than strictly local distribution. TTFIELDS distribute throughout large regions of the brain in a heterogeneous manner.^{5,27} Consequently, TTFIELDS are directed towards regions of brain that include not only the tumor bed, but also the adjacent brain tissue

containing infiltrating tumor cells. Therefore, TTFIELDS represent a spatial complement to radiation, addressing both microscopic neoplastic infiltration into surrounding normal-appearing brain tissue²⁸ as well as local disease and potentially also tumor initiating cells. TTFIELDS can be used effectively to address larger volumes, as they have a low toxicity profile, with no known effect on the normal brain. This is in contrast to increasing doses of radiation (e.g., >60Gy) that lead to risk of radiation necrosis.

There are some limitations to our analyses: Primarily, this analysis is an unplanned retrospective analysis of patients in the EF-14 trial that exhibited radiographic progression. At the time of database closure only 60% of patients had progressed, thus limiting the sample size. However, the demographics of the groups compared in this study remain well-balanced (Table 1).

A second limitation to this study is that distant progression was only observed in a small number of patients treated with RT+TMZ followed by TMZ adjuvant treatment (the TMZ alone group in the EF-14 trial) which results in a large level statistical uncertainty when determining the rate of distant progression within this group. However, as discussed above, other studies have reported similar rates of distant progression in GBM patients treated with RT+TMZ, lending support to the validity of the rates measured in this study. Despite the small numbers, our analysis shows that the rates of distant progression in the TMZ alone and TTFIELDS plus TMZ groups of this study are statistically significant, further supporting the claim that adding TTFIELDS to treatment alters the pattern of GBM progression.

Finally, in this study we investigated progression patterns by contouring enhancing tumor identified on T1c MRIs at baseline (after end of chemoradiotherapy) and at progression, and thus did not utilize all available imaging data in the analysis. Utilization of all available imaging data including T2 and FLAIR images as well as inclusion of additional

time-points into the analysis would enable a more refined distinction between different regions of the tumor. It would also potentially enable finer distinction between progression and pseudo-progression when classifying regions of enhancement in close proximity to the primary lesion. Notably, it would also enable a dynamic description of how the tumors progress over time and how TTFIELDS influence various regions of the tumor including regions of non-enhancing tumor and surrounding edema. Performing such an analysis utilizing “human MRI readers” is possible. However, since the task is labor intensive it would require multiple readers. The use of multiple readers in itself may introduce inter-reader variability into the analysis. Hence, a more practical and methodological approach to performing such a study may be to utilize substantial computing power, in conjunction with sophisticated standardized imaging algorithms.

The results of our analysis show that the addition of TTFIELDS to adjuvant TMZ changes the progression pattern of GBM, and demonstrates a direct correlation between TTFIELDS dose distribution and tumor progression. These results confirm the therapeutic activity of TTFIELDS in a dose dependent manner. Optimizing array placement to maximize TTFIELDS dose in areas at highest risk of progression as well as adapting array layout after tumor progression is a viable and important strategy to optimize outcomes for GBM patients.

References

1. Kirson ED, Gurvich Z, Schneiderman R, et al. Disruption of cancer cell replication by alternating electric fields. *Cancer Res.* 2004;64(9):3288-3295.
2. Kirson ED, Dbaly V, Tovarys F, et al. Alternating electric fields arrest cell proliferation in animal tumor models and human brain tumors. *Proc Nat Acad Sci U S A.* 2007;104(24):10152-10157.

3. Giladi M, Schneiderman RS, Voloshin T, et al. Mitotic Spindle Disruption by Alternating Electric Fields Leads to Improper Chromosome Segregation and Mitotic Catastrophe in Cancer Cells. *Sci Rep*. 2015;5:18046.
4. Porat Y, Giladi M, Schneiderman RS, et al. Determining the Optimal Inhibitory Frequency for Cancerous Cells Using Tumor Treating Fields (TTFields). *J Vis Exp* . 2017;123:55820.
5. Wenger C, Salvador R, Basser PJ, Miranda PC. Improving Tumor Treating Fields Treatment Efficacy in Patients With Glioblastoma Using Personalized Array Layouts. *Int J Radiat Oncol Biol Phys*. 2016;94(5):1137-1143.
6. Chaudhry A, Benson L, Varshaver M, et al. NovoTTF-100A System (Tumor Treating Fields) transducer array layout planning for glioblastoma: a NovoTAL system user study. *World J Surg Oncol*. 2015;13:316.
7. Toms SA, Kim CY, Nicholas G, Ram Z. Increased compliance with tumor treating fields therapy is prognostic for improved survival in the treatment of glioblastoma: a subgroup analysis of the EF-14 phase III trial. *J Neurooncol*. 2019;141(2):467-473.
8. Stupp R, Taillibert S, Kanner A, et al. Effect of tumor-treating fields plus maintenance temozolomide vs maintenance temozolomide alone on survival in patients with glioblastoma: A randomized clinical trial. *JAMA*. 2017;318(23):2306-2316.
9. Ballo MT, Urman N, Lavy-Shahaf G, Grewal J, Bomzon Z, Toms S. Correlation of Tumor Treating Fields Dosimetry to Survival Outcomes in Newly Diagnosed Glioblastoma: A Large-Scale Numerical Simulation-Based Analysis of Data from the Phase 3 EF-14 Randomized Trial. *Int J Radiat Oncol Biol Phys*. 2019;104(5):1106-1113.
10. Taphoorn MJB, Dirven L, Kanner AA, et al. Influence of Treatment With Tumor-Treating Fields on Health-Related Quality of Life of Patients With Newly Diagnosed Glioblastoma: A Secondary Analysis of a Randomized Clinical Trial. *JAMA Oncol*. 2018;4(4):495-504.
11. Ashburner J. SPM: A history. *Neuroimage*. 2012;62(2):791-800.

12. Yushkevich PA, Piven J, Hazlett HC, et al. User-guided 3D active contour segmentation of anatomical structures: significantly improved efficiency and reliability. *Neuroimage*. 2006;31(3):1116-1128.
13. Piper RJ, Senthil KK, Yan JL, Price SJ. Neuroimaging classification of progression patterns in glioblastoma: a systematic review. *J Neurooncol*. 2018;139(1):77-88.
14. Verma G, Chawla S, Mohan S, et al. Three-dimensional echo planar spectroscopic imaging for differentiation of true progression from pseudoprogression in patients with glioblastoma. *NMR Biomed*. 2019;32(2):e4042.
15. Zhang K, Wang XQ, Zhou B, Zhang L. The prognostic value of MGMT promoter methylation in Glioblastoma multiforme: a meta-analysis. *Fam Cancer*. 2013;12(3):449-458.
16. Jiang H, Yu K, Li M, et al. Classification of Progression Patterns in Glioblastoma: Analysis of Predictive Factors and Clinical Implications. *Front Oncol*. 2020;10:590648.
17. Ballo MT, Urman N, Bomzon Z, Lavy-Shahaf G, Toms S. Increasing Tumor Treating Fields dose at the tumor bed improves survival: Setting a framework for TTFIELDS dosimetry based on analysis of the EF-14 Phase III trial in newly diagnosed glioblastoma. *Cancer Res*. 2019;79(13 Suppl): Abstract nr CT204.
18. Scherer HJ. Structural development in gliomas. *Am J Cancer*. 1938;34(3):333-351.
19. Scherer HJ. The forms of growth in gliomas and their practical significance. *Brain*. 1940;63(1):1-35.
20. Sahm F, Capper D, Jeibmann A, et al. Addressing diffuse gliomas as a systemic brain disease with single cell analysis. *Arch Neurol*. 2012;69(4):523-526.
21. Drumm MR, Dixit KS, Grimm S, et al. Extensive brainstem infiltration, not mass effect, is a common feature of end-stage cerebral glioblastomas. *Neuro Oncol*. 2020;22(4):470-479.
22. Chan JL, Lee SW, Fraass BA, et al. Survival and failure patterns of high-grade gliomas after three-dimensional conformal radiotherapy. *J Clin Oncol*. 2002;20(6):1635-1642.

23. Paulsson AK, McMullen KP, Peiffer AM, et al. Limited margins using modern radiotherapy techniques does not increase marginal failure rate of glioblastoma. *Am J Clin Oncol*. 2014;37(2):177-181.
24. Gebhardt BJ, Dobelbower MC, Ennis WH, Bag AK, Markert JM, Fiveash JB. Patterns of failure for glioblastoma multiforme following limited-margin radiation and concurrent temozolomide. *Radiat Oncol*. 2014;9:130.
25. Brandes AA, Tosoni A, Franceschi E, et al. Recurrence pattern after temozolomide concomitant with and adjuvant to radiotherapy in newly diagnosed patients with glioblastoma: correlation With MGMT promoter methylation status. *J Clin Oncol*. 2009;27(8):1275-1279.
26. Vymazal J, Wong ET. Response patterns of recurrent glioblastomas treated with tumor-treating fields. *Semin Oncol*. 2014;41(Suppl 6):S14-24.
27. Wenger C, Miranda PC, Salvador R, et al. A Review on Tumor-Treating Fields (TTFields): Clinical Implications Inferred From Computational Modeling. *IEEE Rev Biomed Eng*. 2018;11:195-207.
28. Chawla S, Wang S, Asadollahi S, Nasrallah M, Bagley S, Desai A, Desiderio L, Brem S, Poptani H, Mohan S. Assessment of Safety Profile of Tumor Treating Fields on Normal Brain in Glioblastoma Patients Using Diffusion Tensor Imaging. *Radiological Society of North America 2019 Scientific Assembly and Annual Meeting*. Chicago IL, 2019.

Figure 1: EF-14 Patient MRI Data Flow for Progression Analysis

Figure 2: Kaplan Meier curves showing OS and PFS when splitting the patient population according to progression type (a) PFS of TTFIELDS plus TMZ treated patient, (b) PFS of TMZ alone patients, (c) OS of TTFIELDS plus TMZ treated patient, (d) OS of TMZ alone patients.

Figure 3: Representative TTFIELDS distribution dose maps

(a) Patient with both regression and local progression: (i) Baseline MRI. (ii) Baseline MRI with segmented baseline volumes: GTV (red), and 3mm PBZ around baseline tumor (yellow). (iii) Progression MRI. (iv) Progression MRI with segmented volumes: tumor to tumor (red), necrotic core (cyan), tumor to norm (green), and norm to norm (yellow). (v) TTFIELDS dose density map with volumes contours overlaid.

(b) Patient exhibited distant progression (marked with a white circle in the axial slice) and local regression: (i+ii) Baseline MRI. (iii) Baseline MRI with segmented baseline volumes: GTV (red), necrotic core (cyan), and 3mm PBZ around baseline tumor (yellow). (iv+v) Progression MRI. (vi) Progression MRI with segmented volumes: tumor to tumor (red), necrotic core (cyan), norm to norm (yellow), and tumor to norm (green). (vii) TTFIELDS dose density map with volumes contours overlaid.

(c) Patient with infra-tentorial progression: (i) Baseline MRI. (ii) Baseline MRI with segmented baseline volumes: GTV (red), resection cavity (cyan), and 3mm PBZ around baseline tumor (yellow). (iii) Progression MRI. (iv) Progression MRI with segmented volumes: tumor to norm (green), norm to norm (yellow), normal to tumor (red), and necrotic core (cyan). (v) TTFIELDS dose density map with volumes contours overlaid.

Table 1: Patient Demographics for tumor progression analysis

Characteristics	TFields plus TMZ (N=306)	TMZ alone (N=122)	p-Value ¹
Age (Years)			
N	306	122	
Median (range)	56.0 (19-83)	57.5 (22-78)	
Sex, No. (%)			
Male	209 (68.3%)	87 (71.3%)	0.543
Female	97 (31.7%)	35 (28.7%)	
Region, No. (%)			
United States	145 (47.4%)	55 (45.1%)	0.666
Rest of world	161 (52.6%)	67 (54.9%)	
Extent of Resection, No. (%)			
Biopsy	41 (13.4%)	16 (13.1%)	0.952
Partial Resection	98 (32.0%)	41 (33.6%)	
Gross Total Resection	167 (54.6%)	65 (53.3%)	
MGMT Tissue available and tested, No. (%)	257 (84.0%)	106 (86.9%)	
Methylated	85 (33.1%)	32 (30.2%)	0.825
Unmethylated	149 (58.0%)	63 (59.4%)	
Invalid	23 (8.9%)	11 (10.4%)	
Tumor Position, No. (%)			
Corpus Callosum	21 (6.9%)	6 (4.9%)	0.342
Frontal Lobe	128 (41.8%)	42 (34.4%)	
Occipital Lobe	33 (10.8%)	17 (13.9%)	
Parietal Lobe	88 (28.8%)	49 (40.2%)	
Temporal Lobe	130 (42.5%)	54 (44.3%)	
Missing	2 (0.7%)	1 (0.8%)	
Tumor Location, No. (%)			
Left	139 (45.4%)	53 (43.4%)	0.800
Right	165 (53.9%)	67 (54.9%)	
Both	2 (0.7%)	2 (1.6%)	
Corpus Callosum	12 (3.9%)	5 (4.1%)	
Completed radiation therapy, No. (%)			
<57 Gy	14 (4.6%)	6 (4.9%)	0.837
60 Gy (standard; ±5%)	280 (91.5%)	111 (91.0%)	
>63 Gy	11 (3.6%)	3 (2.5%)	
Concomitant temozolomide use, No. (%)			

Characteristics	TTFIELDS plus TMZ (N=306)	TMZ alone (N=122)	p-Value ¹
Yes	287 (93.8%)	115 (94.3%)	0.854
Unknown	19 (6.2%)	7 (5.7%)	
Karnofsky Performance Score			
Median (range)	90 (60-100)	90 (70-100)	

¹ Chi-squared test for percentage values and T test for means values

Table 2: TTFIELDS Dose to brain volumes within the PBZ expansion margins

PBZ Expansion margin (mm)	Number of patients	<i>avg</i> TTFIELDS Dose in norm to norm (<i>mW/cm3</i>)	<i>avg</i> TTFIELDS Dose in norm to tumor (<i>mW/cm3</i>)	Difference (<i>mW/cm3</i>)	p-value t-test
3	233	0.792	0.731	0.061	<0.001
5	233	0.783	0.732	0.051	<0.001
10	239	0.779	0.734	0.044	0.001
15	240	0.77	0.73	0.041	0.003
20	243	0.765	0.726	0.039	0.005

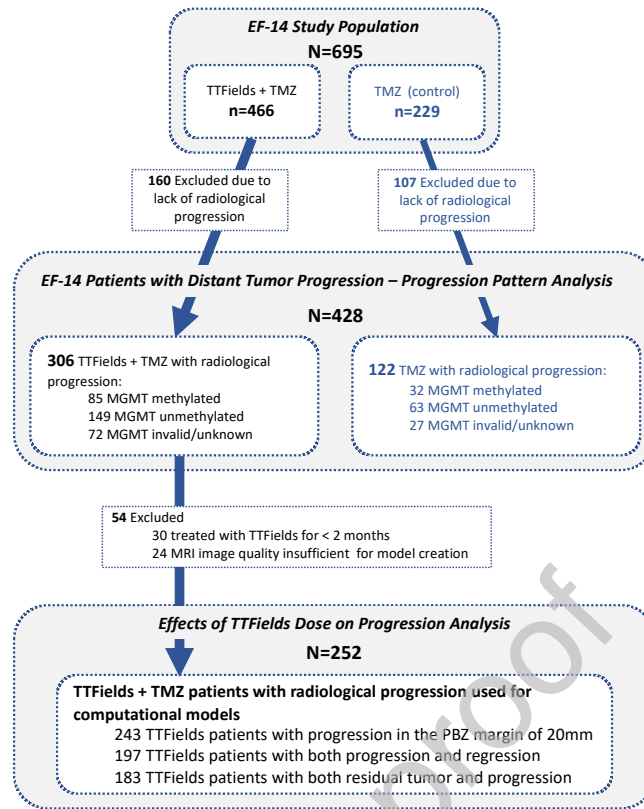
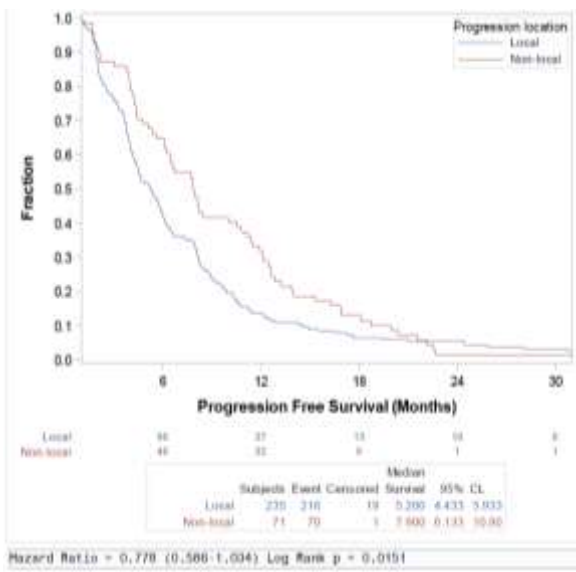
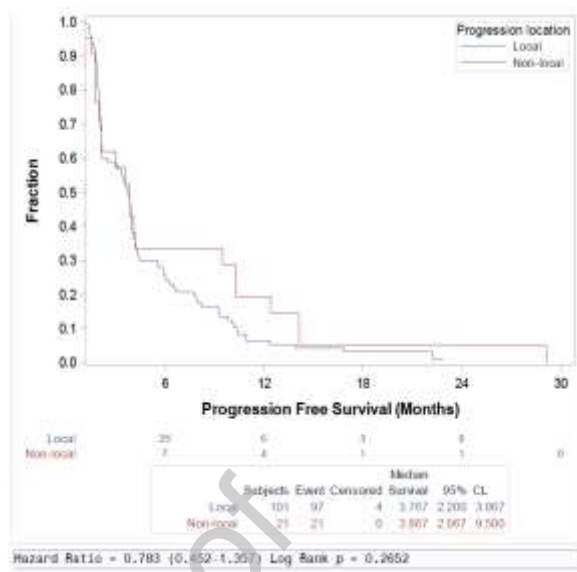


Figure 1: EF-14 Patient MRI Data Flow for Progression Analysis

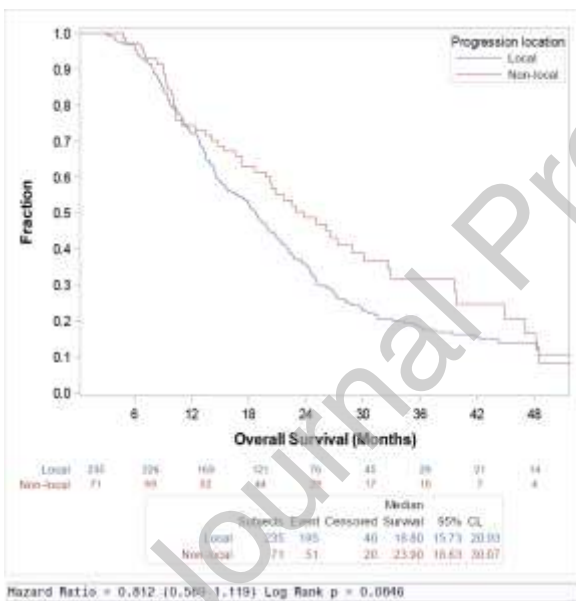
(a) TTFields Progression free survival



(b) Control Progression free survival



(c) TTFields Overall survival



(d) Control Overall survival

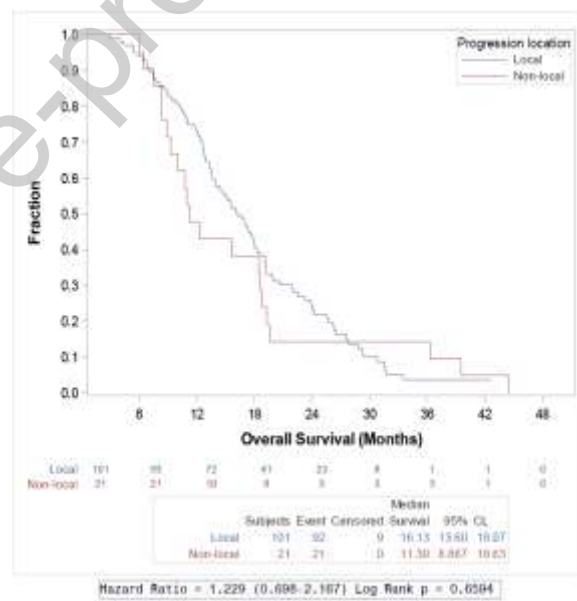
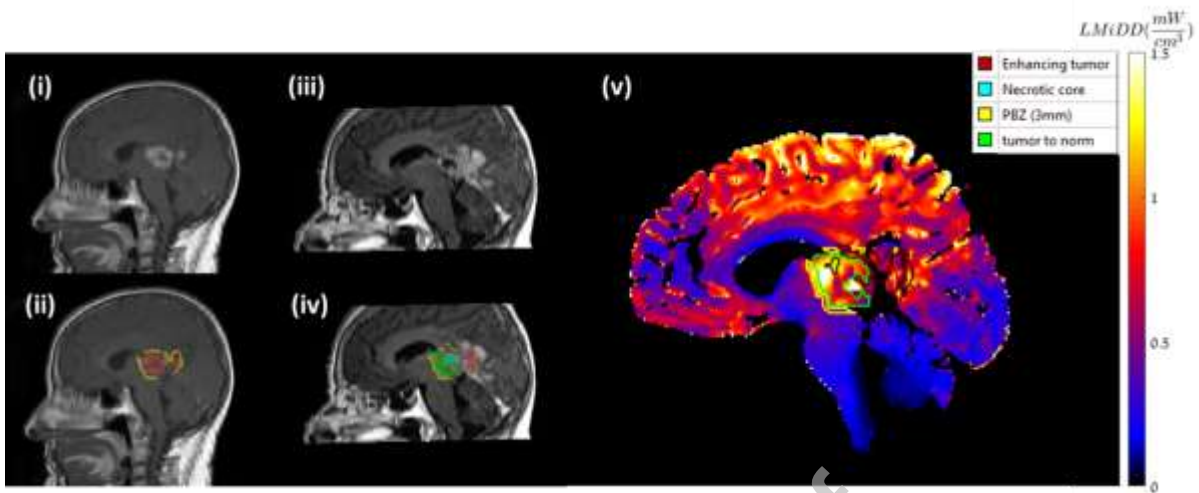
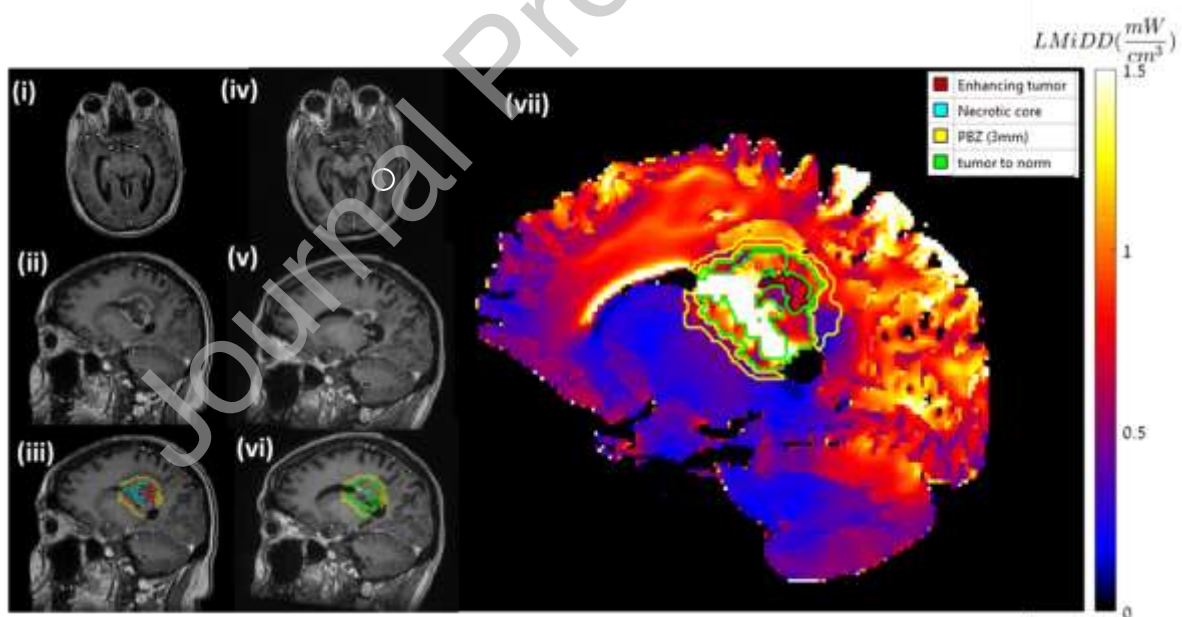


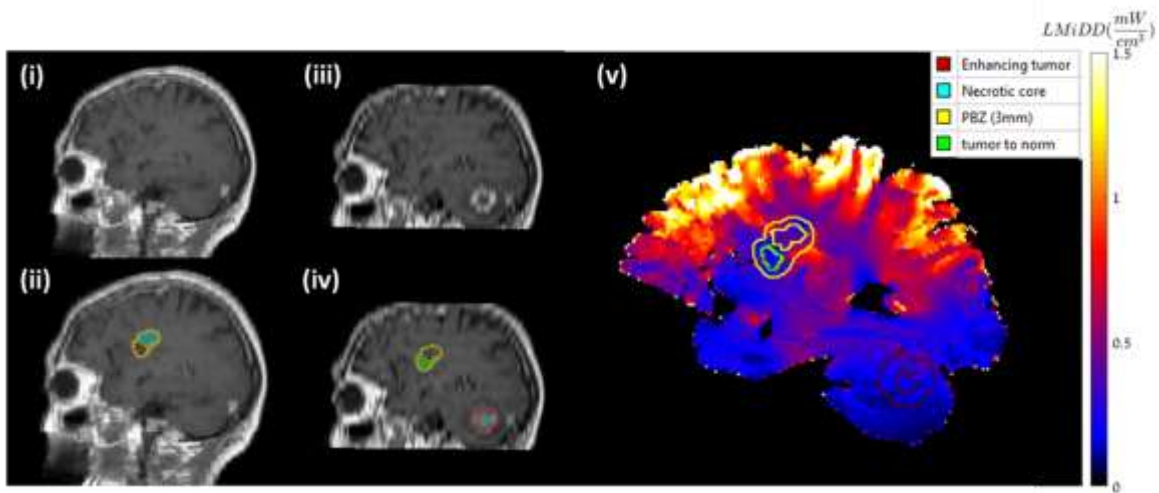
Figure 2: Kaplan Meier curves showing OS and PFS when splitting the patient population according to progression type (a) PFS of TTFields plus TMZ treated patient, (b) PFS of TMZ alone patients, (c) OS of TTFields plus TMZ treated patient, (d) OS of TMZ alone patients.

Figure 3: Representative TTFields distribution dose maps

(a) Patient with both regression and local progression: (i) Baseline MRI. (ii) Baseline MRI with segmented baseline volumes: GTV (red), and 3mm PBZ around baseline tumor (yellow). (iii) Progression MRI. (iv) Progression MRI with segmented volumes: tumor to tumor (red), necrotic core (cyan), tumor to norm (green), and norm to norm (yellow). (v) TTFields dose density map with volumes contours overlaid.



(b) Patient exhibited distant progression (marked with a white circle in the axial slice) and local regression: (i-ii) Baseline MRI. (iii) Baseline MRI with segmented baseline volumes: GTV (red), necrotic core (cyan), and 3mm PBZ around baseline tumor (yellow). (iv+v) Progression MRI. (vi) Progression MRI with segmented volumes: tumor to tumor (red), necrotic core (cyan), norm to norm (yellow), and tumor to norm (green). (vii) TTFields dose density map with volumes contours overlaid.



(c) Patient with infra-tentorial progression: (i) Baseline MRI. (ii) Baseline MRI with segmented baseline volumes: GTV (red), resection cavity (cyan), and 3mm PBZ around baseline tumor (yellow). (iii) Progression MRI. (iv) Progression MRI with segmented volumes: tumor to norm (green), norm to norm (yellow), normal to tumor (red), and necrotic core (cyan). (v) TTFIELDS dose density map with volumes contours overlaid.